Crystallinity and Microstructure of Plasticized Poly(vinyl chloride). A ^{13}C and ^{1}H Solid State NMR Study

W. Barendswaard,* V. M. Litvinov, F. Souren, and R. L. Scherrenberg

DSM Research, P.O. Box 18, 6160 MD Geleen, The Netherlands

C. Gondard and C. Colemonts

Limburgse Vinyl Maatschappij, H. Hartlaan, 3980 Tessenderlo, Belgium

Received October 14, 1997; Revised Manuscript Received August 20, 1998

ABSTRACT: The combination of ^{13}C solution NMR and ^{13}C solid-state NMR (CP/MAS and MAS) is used to reveal the relative amount of rigid (crystalline) PVC in two PVC/DOP (50/50 wt % of poly(vinyl chloride)/di-2-ethylhexyl phthalate) samples with tacticities, α, of 0.52 and 0.575, respectively. For both samples the crystallinity decreases with increasing temperature, from about 30% at 90 °C to approximately 6% at 180 °C. By means of a careful spectral deconvolution of the ^{13}C solid-state NMR spectra, the relative amounts of different triad sequences in the crystallites of PVC were obtained. The relative fractions of *rr* and *rm* sequences, about 0.5 and 0.4 respectively, are found to be constant as a function of temperatures above 90 °C. On the basis of proton low resolution T_2 experiments the mean average amorphous chain length between crystals was estimated at 50 monomer units at 160−180 °C. All results can be well understood by assuming the existence of crystallites which on average consist of only a few syndiotactic sequences in the chain direction.

1. Introduction

More than 50 years after the first commercial production of PVC, the relations between the (micro)morphology of PVC and its final properties are still not fully understood. This lack of understanding is largely due to the complex structure of PVC, combined with various experimental problems concerning the characterization of the microstructure in PVC. One of the problems is the determination of the degree of crystallinity.

The results of the traditional methods for crystallinity determination, such as density measurements[1], Infrared spectroscopy[2], Wide angle X-ray scattering (WAXS),[3] and differential scanning calorimetry (DSC)[4] are difficult to interpret on this point although rough estimates can be obtained.

On the basis of various DSC and WAXS experiments it has been proposed[5,6,7] that PVC is composed of "pseudo crystals" which differ widely in perfection and size, causing a wide melting range. One of the main questions which thereby arises concerns is the actual size and tacticity of the crystallites.[8] It has been proposed by some authors that crystallites in PVC are very small and are primarily ordered perpendicular to the polymer backbone.[7,9−11] The average thickness of these plates is not well-known but estimates range between 7 and 15 Å.[10,12] Some authors assume that the crystallites contain only syndiotactic "*rr*" (racemic) sequences,[6,11,13,14] whereas others, on the basis of molecular modeling, have proposed that an even amount of *m* (meso) sequences can also be incorporated into the crystallites.[15,16]

However, none of the pictures described above could completely be proved because the afore-mentioned techniques fail to present a clear picture of the micromorphological organization of PVC. In this article ^{13}C and ^{1}H solid-state NMR techniques are employed to investigate the (micro)morphology of semicrystalline, plasticized PVC in relation to chain tacticity. In section 3.1 ^{13}C CP/MAS experiments are described which have been performed as a function of contact time over a wide temperature range in order to identify the different phases in PVC. In section 3.2 quantification of these phases (at different temperatures) was performed using ^{13}C single pulse experiments. Section 3.3 deals with several low resolution ^{1}H relaxation NMR experiments aiming at the determination of the average (amorphous) chain length between crystals. It is suggested that at elevated temperatures, PVC can be regarded as an elastomer network in which the crystallites act as cross-links. In section 4 (discussion) it is first shown that all NMR results are in agreement with a two-phase (amorphous/crystalline) picture of PVC. Second, by combining the results of the different NMR experiments, information about the crystallinity of plasticized PVC as a function of temperature and about the size and the nature of the crystalline and amorphous phases in terms of tacticity could be obtained.

Finally, a simplified micromorphological picture of PVC is proposed on the basis of chain statistics as used in Flory's model on the crystallization of copolymers and on the NMR results. This picture is in agreement with the assumptions of a small crystallite size along the chain direction and the crystallites being composed of only syndiotactic sequences.

2. Experiment and Theory

2.1. Samples. For this study plasticized PVC was used since it was found that the much larger mobility differences between the crystalline and amorphous fractions in this material, as compared to nonplasticized PVC, facilitates the interpretation of the solid-state NMR results. Moreover, plasticizer contents of up to 50 wt % do not seem to affect the structural order of PVC.[9]

Two PVC samples containing 50% of the plasticizer DOP (di-2-ethylhexyl phthalate) were investigated: one had a molar mass of about 60×10^3 g/mol (sample 1; Marvylan S7102 (Kv71); tacticity $\alpha = 0.52$) whereas the other had a molar mass of 85×10^3 g/mol (sample 2; laboratory sample provided by

10.1021/ma971508y CCC: $18.00
Published on Web 12/18/1998

LVM (Kv99); tacticity $\alpha = 0.575$).[8] The α value here represents the overall chain fraction of syndiotactic sequences in the polymer chain. Both PVC/DOP samples were thermally stabilized with 3 wt % of dibasic lead stearate (Harochem P51 from AKRCOS) because of the experiments at high temperatures.

In the course of the ^{1}H relaxation experiments, an additional sample was studied as a reference for amorphous PVC: a random vinyl acetate−vinyl chloride copolymer (PVC/VA) (8 mol % vinyl acetate; Lucovyl E428 from Atochem) stabilized with 2 phr 17 MOK (dioctylstannum bis(isooctylmercaptoacetate)).

With the exception of the vinyl acetate−vinyl chloride copolymer sample, which was prepared from a cast film, the plasticized PVC/DOP samples were processed in a roll mill at 170 °C for several minutes in order to obtain a homogeneous distribution of the DOP.

2.2. NMR Experiments. The ^{13}C NMR spectra of PVC solutions were recorded at 110 °C on a Varian Unity 300 spectrometer equipped with a 10 *mm* ^{13}C Varian probe using a 90° excitation pulse of 15μs and a waiting time of 5 s. The solvent used was $C_2D_2Cl_4$.[17]

All ^{13}C solid-state NMR experiments were carried out with a Varian Unity 400WB spectrometer equipped with a Varian 7 *mm* variable temperature CP/MAS probe. Typical MAS spinning rates were 4000 Hz. The CP/MAS spectra at different cross-polarization times were recorded as a function of temperature in the range 20−180 °C. The waiting time in the single pulse experiments was varied from 2 up to 50 s, which is long with respect to the T_1's of the different carbons (10−15 s, as determined by means of the Torchia sequence[18]). The length of a 90° ^{13}C pulse was set to 12 μs in all experiments, while the decoupling power was about 40 kHz. Because of the narrow spectral range of the PVC resonances, the relative intensities of the resonances are not affected by the relatively long 90° pulse length as was found by a reference experiment with a 90° pulse length of 5 μs.

Prior to the ^{13}C experiments, the samples were kept at 200 °C for 2 min and subsequently cooled to room temperature at a rate of about 50 °C/min in order to match their thermal histories. After cooling to room temperature, the samples were stepwise heated, and solid-state NMR experiments were performed at different temperatures up to 165 (sample 1) or 180 °C (sample 2). To avoid annealing effects during the measurements, the samples were kept at each temperature for about 30 min before the experiments were started. The NMR measuring time at a certain temperature was in the range between 6 and 24 h for the ^{13}C (CP)MAS experiments and about 2 h for the ^{1}H relaxation experiments. To detect a possible influence of the thermal treatment of the sample on the NMR parameters, one of the samples (sample 2) was, after the last experiments at 180 °C had been performed and the sample had been cooled to room temperature, again heated to 120 °C, and the original ^{13}C measurements at this temperature were repeated. Since the results of these second experiments are identical, within experimental error, to those of the original experiments, they will not be discussed separately in section 3. Despite their prolonged exposure to elevated temperatures the samples showed only a slight coloring.

Low resolution proton T_2 NMR relaxation experiments were carried out on a Bruker 20 MHz Minispec spectrometer. This spectrometer was equipped with a home-built variable temperature unit for measurements in the range of −100 to +200 °C. T_2 values below 50−100 μs were determined by a solid-echo pulse sequence, whereas the longer relaxation times were measured with a Hahn-echo sequence. The solid-echo pulse sequence ($90_x°-\tau-90_y°-\tau-$acq) with $\tau = 20$ μs was used to record the transverse magnetization decay of both the rigid and the mobile PVC fraction in the samples. The length of the 90° pulse combined with the relatively long "dead time" of the spectrometer used was 18μs. The Hahn-echo pulse sequence ($90_x°-\tau-180_x°-\tau-$acq) was used for an accurate determination of the ^{1}H T_2 relaxation time for the amorphous phase of PVC and of the DOP. The echo height was determined as a function of 2τ. Both the solid-echo and the Hahn-echo decays were acquired using a 90° pulse length of 8 μs.

2.3. Data Analysis. 2.3.1. ^{13}C Experiments. All ^{13}C solid-state spectra were fitted with a software program developed in our laboratory.[19] This program is based on the least squares parameter adjustment criterion of spectra using the Levenberg−Marquardt iteration procedure.[20] The program is not only capable of fitting a single spectrum (1D fit) but can also be used to obtain a best fit of an array of spectra ("2D fits"). The 2D fit adjusts one peak position, one line shape (a Lorenz/Gauss ratio whereby 0 represents a Gaussian and 1 represents a pure Lorentzian) and one line width for a peak appearing in (a number of) the spectra in the array in such a way that a best fit for the array of spectra is obtained. The important improvement of a 2D fit as compared with a 1D best fit is therefore an improved reliability of the obtained "best fit" parameter values. The program calculates an F value which provides information about the statistical relevance of the fits. The statistical relevance is expressed by the F value obtained from the Fisher test. In some cases, the uncertainties in the parameter values are estimated on the basis of a systematic variation (and subsequent fixation) of input parameter values. The program finally numerically calculates the integral intensity of each adjusted peak on the basis of the intensity, width, and line shape.

For the analysis of the ^{13}C CP/MAS experiments as a function of cross-polarization time, the peak intensities ($H(t)$) obtained from the 2D fit program were least-squares adjusted to eq 1[21]

$$H(t) = H_0[\exp(-t/T_{1\rho}(^1\mathrm{H}) - \exp(-t/T_{\mathrm{CH}})] \qquad (1)$$

where H_o is the maximum ^{13}C magnetization which can be obtained during cross-polarization, T_{CH} represents the characteristic time for the build up of the carbon magnetization and $T_{1\rho}(^1\mathrm{H})$ represents the characteristic decay time of the proton magnetization in the spin-locked state. It is assumed here not only that $T_{CH} \ll T_{1\rho}(^{13}\mathrm{C})$ (carbon-13 relaxation time in the rotating frame) but also that $T_{CH} \ll T_{1\rho}(^1\mathrm{H})$.

2.3.2. ^{1}H Experiments. Proton decays of the transverse magnetization were analyzed by least-squares adjusting the parameters of an optional decay function, such as an exponential function, a Weibull function, a log-normal distribution of exponents, and a function based on the theory of transverse relaxation in elastomeric networks,[22] hereafter referred to as the Cohen−Addad function, or of a combination of these functions. In the presentation of the results, only the statistically most relevant descriptions of the proton relaxation decays are presented. The time constants of these functions are given by the T_2 relaxation time, whereas the relative intensities of the relaxation components are proportional to the fraction of protons in different (micro)phases characterized by different T_2 values. In our case, with 50/50 wt % PVC/DOP samples, the proton fraction of PVC amounts to 0.33.

2.4. Theoretical Background for ^{1}H Experiments. A quantitative interpretation of the ^{1}H T_2 value with respect to the mean average chain length between crystallites was carried out for PVC samples above 165 °C, where the crystallinity is low. In this case PVC could be considered as a physical network[9,23,24] in which small crystallites act as cross-links which are permanent on the time scale of the NMR experiment. The T_2 value for elastomer networks is quantitatively related to the number of statistical segments between chemical cross-links and chain entanglements at temperatures about 100−150 °C above the glass transition temperature (at the time scale of the T_2 experiments, i.e., 1−10 kHz).[25−27,38] This determination of cross-link density is based on the assumption of the validity of Gaussian chain statistics (number of rotatable backbone bonds ≥ 50). The following equation relates the T_2 value to the number of statistical segments between cross-links:[25,26]

$$T_2^{\mathrm{p}} = a(T_2^{\mathrm{rl}})Z \qquad (2)$$

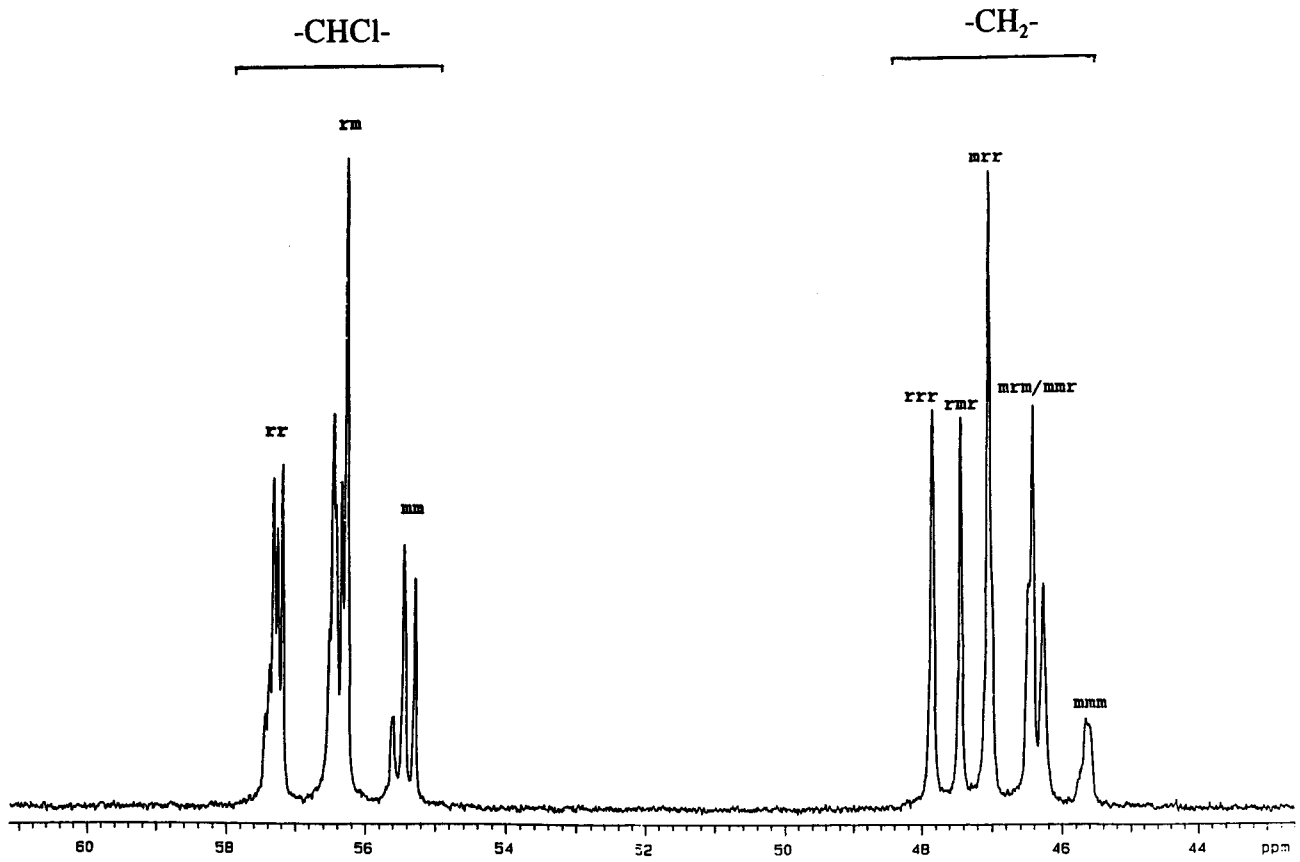

Figure 1. ^{13}C NMR spectrum at 110 °C of sample 1, dissolved in $C_2D_2Cl_4$.

Here T_2^p is the observed plateau value at (T_g^{NMR} + 150 °C)[25,26] and T_2^{rl} represents the T_2 value for a "rigid" chain below T_g which is at about −20 °C for the PVC/DOP samples studied. A T_2^{rl} of 14.4 μs for pure PVC was determined at −75 °C. In eq 2, a is a coefficient, which has a value of about 6.2 for aliphatic chains.[25,26] Z is the number of statistical segments between cross-links and is related to M_c, the molar mass of the network chains, by

$$M_c = ZC_\infty M_u/n \quad (3)$$

In eq 3 M_u represents the molar mass per elementary chain unit, n is the number of rotatable backbone bonds in an elementary chain unit and C_∞ is the number of rotatable backbone bonds of the statistical segment. A value of 6.7 for C_∞ was taken for the M_c calculation.[28] Equation 2 is valid for moderately cross-linked networks, which limits its application to PVC with a very low amount of crystallinity or to (elevated) temperatures at which the crystallinity of PVC is relatively low (5−10%). The interchain entanglements arising from crystallites are assumed to be of minor importance in this case.

3. Results

Figure 1 shows a ^{13}C spectrum of sample 1 dissolved in $C_2D_2Cl_4$.

The different peaks in the −CHCl− region (around 56.5 ppm) as well as those in the $-CH_2-$ region (around 47 ppm) arise from the different triad and tetrad stereo sequences, respectively.[29] The assignments of the peaks in terms of *r* (racemic) and *m* (meso) are indicated in the figure. From the relative integrated intensity of each of the three groups of peaks in the −CHCl− region (around 55.5, 56.4, and 57.3 ppm) the relative quantity of the *rr*, *rm*, and *mm* triad stereo sequences in the two samples can be obtained; see Table 1.

3.1. Cross-Polarization Experiments. In Figure 2 the $^1H-^{13}C$ cross-polarization (MAS) spectra of sample 1, obtained with a cross-polarization time of 1000 μs, are presented as a function of temperature between 23 and 150 °C. In the spectra the resonances originating from DOP are marked by an asterisk, and it is seen that with increasing temperature these resonances narrow significantly.

Table 1. Fractions of the Triad Stereosequences as Determined from ^{13}C Spectra of the Two PVC/DOP Samples in Solution

	rr	*rm*	*mm*
sample 1	0.305	0.490	0.205
sample 2	0.331	0.488	0.181

According to the NMR spectrum in solution, the PVC resonances at about 47 ppm in the ^{13}C CP/MAS spectra originate from $-CH_2-$ and those at 58 ppm from −CHCl−.[17] At room temperature only two broad PVC resonances are present at 47 and 58 ppm. These broad resonances remain present up to at least 150 °C although their intensity is strongly decreased at this temperature, as will be shown below. At about 60 °C additional, more narrow resonances appear in both the −CHCl− and $-CH_2-$ regions. These additional resonances narrow strongly as the temperature is further increased until they manifest themselves above about 100 °C as a combination of three peaks around 57 ppm and at least three peaks around 46 ppm. To assign the broad and narrow resonances to a physical and/or chemical structure, the behavior of the different peaks as a function of cross-polarization time was studied at different temperatures in the range 20−180 °C. In Figure 3 some typical results from sample 2 at 23 (Figure 3a) and 150 °C (Figure 3b) are reproduced.

The width and shape of the two broad resonances at 23 °C (Figure 3a) are not seen to change as a function

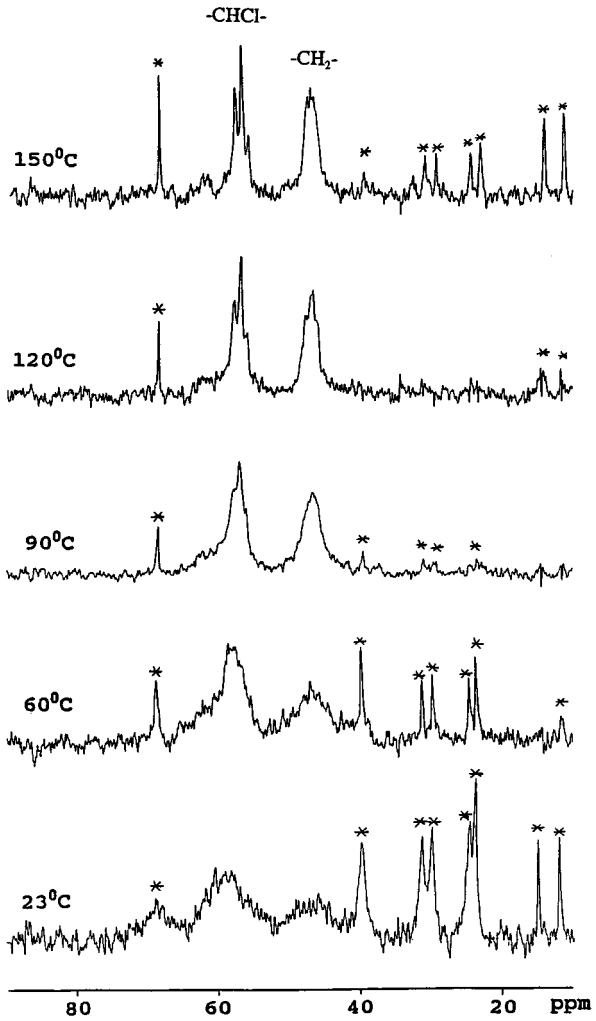

Figure 2. ^{13}C CP/MAS spectra obtained with a 1 ms contact time at different temperatures. The resonances marked by an asterisk are assigned to DOP.

of cross-polarization time. In fact, only two resonances had to be assumed in order to obtain a statistically relevant 2D fit at 23 °C. At 150 °C (parts b and c of Figure 3) three narrow resonances are observed around 57 ppm, and at least five narrow peaks around 46 ppm can be seen at cross-polarization times longer than 1 ms. The two broad resonances can be observed at short cross-polarization times as shown in Figure 3c where three of the spectra from Figure 3b are shown with a vertical multiplication in order to emphasize the broad resonances. For each spectrum in Figure 3c the individual narrow and broad peaks as obtained from the 2D fit are also shown in addition to the overall 2D fits for each spectrum. Despite their relatively low intensity, the large number of spectra used for the 2D fit allows a relatively accurate estimation of the integral intensity of the broad resonances. In Figure 4a, the integral intensity of the broad −CHCl− resonance (as obtained from the 2D fit) is plotted as a function of cross-polarization time (T = 23 °C).

The solid curve in this figure represents a least-squares adjusted best fit to eq 1, from which a very short T_{CH} (16 ± 4 μs) and a $T_{1\rho}(^1H)$ of 1.0 ± 0.2 ms were obtained. From the 2D fit of the ^{13}C CP/MAS spectra at 150 °C (Figure 4b) reliable values of ^{13}C T_{CH} and ^1H $T_{1\rho}$ can be obtained for the broad as well as the narrow resonances, despite their overlap, see parts b and c of Figure 3b. At 150 °C, the broad −CHCl− resonance exhibits T_{CH} and $T_{1\rho}(^1H)$ relaxation times very similar to those obtained at 23 °C.

The line shape of this broad peak is purely Gaussian, and the line width of this peak decreases only slightly with increasing temperature. The narrow peaks, on the other hand, show a distinctly different relaxation behavior, as is seen in Figure 4b. According to the least-squares adjusted parameters of eq 1 (represented by the solid curves in Figure 4b), the three peaks in the −CHCl− region (at 57.6, 56.6, and 55.8 ppm) have not only a much longer T_{CH} (about 1.4, 2.0 and 3.8 ms, respectively) but also significantly longer $T_{1\rho}(^1H)$'s (above 25 ms) compared with the broad resonance. The $T_{1\rho}(^1H)$'s of the narrow peaks increase sharply from about 3 to around 7 ms on raising the temperature from 60 to 90 °C. The $T_{1\rho}(^1H)$ of the broad peak at 58.5 ppm on the other hand is only weakly dependent on the temperature. It is finally noted that the results found for the samples 1 and 2 do not differ significantly.

Although a detailed analyses of the results will be presented in the discussion (section 5), we can already draw some preliminary conclusions here. First, on the basis of the large differences in line width, the T_{CH} and $T_{1\rho}(^1H)$ of the broad and narrow resonances obtained so far, we suggest that two phases with strongly different mobility in PVC/DOP samples are present above about 60 °C. We think that the narrow peaks originate from a mobile phase (mobile on a time scale above about 50−100 kHz), whereas the two broad peaks can be assigned to a rigid phase (rigid on a time scale below 1−10 kHz). The preliminary assignment of the narrow peaks to a mobile phase is based on the relatively long T_{CH} of the narrow resonances and the fact that the $T_{1\rho}(^1H)$ values of the narrow peaks are not equal to each other, an observation which points to the case of a highly mobile phase far above its glass transition where the efficiency of spin diffusion is low.[30] The broad resonances on the other hand exhibit a very short T_{CH} which is indicative of a relatively rigid material.[30] Under the assumption of slow spin diffusion between the two phases, the temperature independence of the $T_{1\rho}1$ (H) of the broad resonances could furthermore originate from a broad distribution of correlation times in the slow or intermediate mobility regime whereas the observed strong temperature dependence of the $T_{1\rho}(^1H)$ of the narrow resonances suggests correlation times in the fast mobility regime. Finally, it is noted that there is a remarkable resemblance between the ^{13}C NMR spectra in solution (Figure 1) and the narrow resonances in ^{13}C solid-state spectra at high temperatures in terms of the positions and number of the narrow −CHCl− peaks. This suggests that the different narrow peaks reflect different triad stereo sequences in the mobile phase.

3.2. Single 90° Pulse Spectra. Single 90° pulse spectra can provide quantitative information about the relative fraction of rigid PVC and about the chain tacticity in the mobile fraction. To determine suitable waiting times for the single pulse experiments, the T_1 values for both the narrow and the broad resonances are determined at three different temperatures, i.e., 23, 90, and 150 °C, by means of Torchia's sequence.[18] The relaxation times of the resonances were found to be relatively invariant as a function of temperature: the T_1 of the broad resonance remains at about 10−15 s whereas the narrow resonances show T_1 times of about

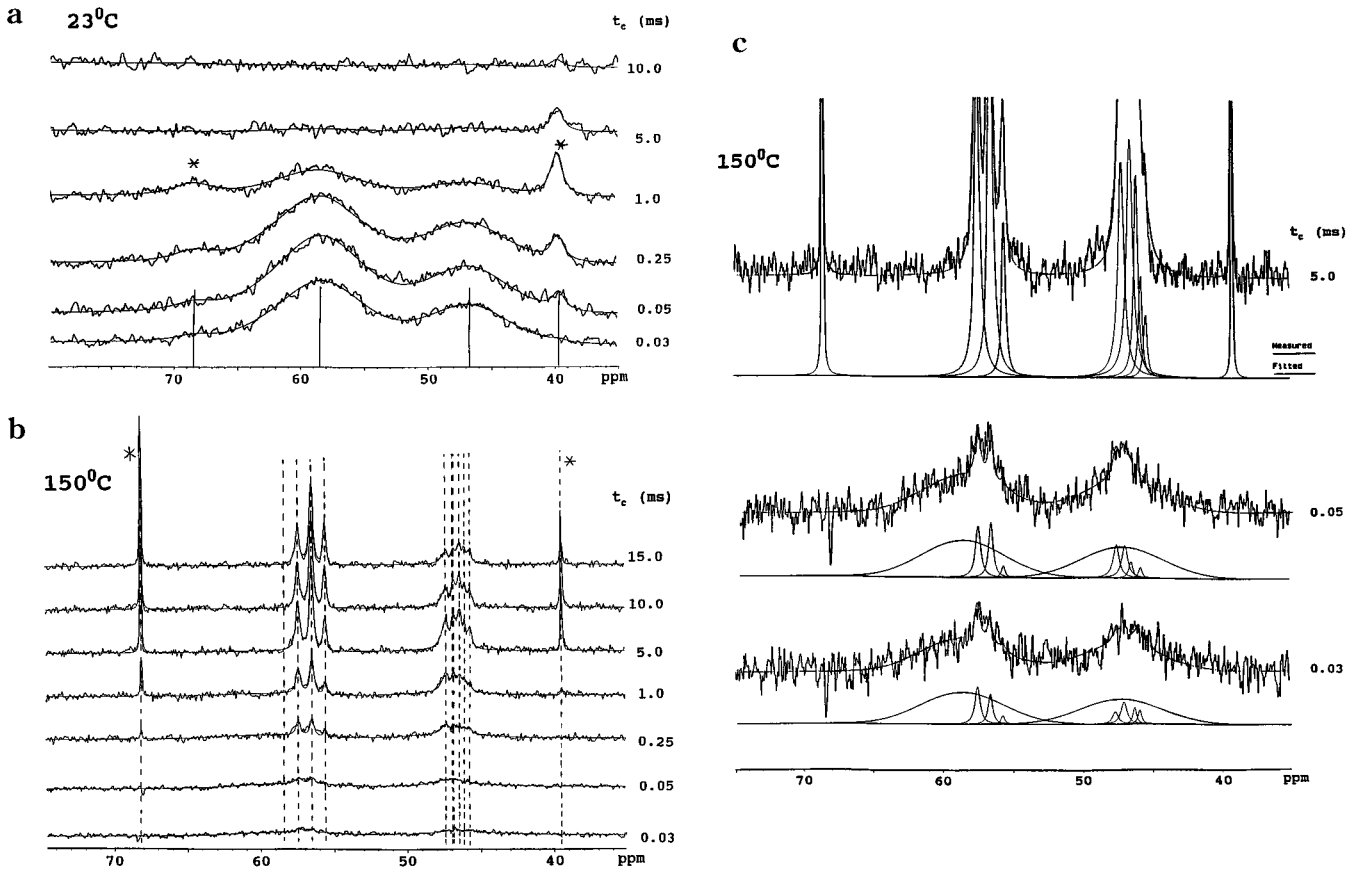

Figure 3. ^{13}C CP/MAS spectra at (a) 23 and (b) 150 °C as a function of contact time. The DOP resonances are marked by an asterisk. The drawn lines in the figures represent the least squares adjusted 2D best fits at the two temperatures. In part c, a five times vertical multiplication of the spectra has been used as compared to part b in order to highlight the presence of the two broad resonances at 58 and 47 ppm at short cross-polarization times. In addition to the overall least squares adjusted 2D best fits for the three spectra in part c, the individual broad and narrow peaks, from which the overall fitted curves originate, are also shown.

1−3 s at 90 and 150 °C. On the basis of these results, 90° pulse HPPD spectra at different temperatures were acquired with an array of waiting times of 20 and 30 s and in most cases also 50 s. The spectra with a waiting time of 50 s are shown in Figure 5a as a function of temperature.

It is seen that above 60 °C the narrow PVC resonances gradually increase in intensity as a function of increasing temperature at the expense of the intensity of the broad PVC resonances. At temperatures above about 120 °C it becomes more difficult to observe the broad resonances due to their low intensity. However, the 2D fits of the CP/MAS spectra at short cross-polarization times clearly indicate that the broad resonances are present at these temperatures (see, e.g., Figure 3b). In the 2D fits of the single pulse spectra, the position, shape, and width of the broad resonances could therefore be fixed to the values obtained from the fits of CP/MAS spectra, leaving the height as the only adjustable parameters for the broad resonance. For the 2D fitting of the narrow peaks in the −CHCl− region at temperatures from 90 to 180 °C, no constraints were imposed. The widths of the narrow resonances decrease from 90 °C up to about 150 °C but remain about constant between 150 and 180 °C. The Lorentz/Gauss ratio of the narrow 55.8 ppm resonance furthermore changes from 1.0 (Lorentz) to 0.0 (Gauss) from 90 to 180 °C, probably because each narrow peak originates from a number of peaks which are very close to each other as observed in the ^{13}C solution NMR spectrum. In this way, reliable quantitative data regarding the fraction of rigid material and the tacticity in the mobile amorphous phase could be obtained. In Figure 5b, the experimental and fitted spectra at 150 °C are reproduced in more detail. Each of the constituent peaks are shown at the bottom whereas the resulting best fit is represented by the continuous line through the experimentally measured spectrum in the upper part of Figure 5b. The integral intensity, as obtained directly from the spectrum, is also shown in Figure 5b. From the curve of the integral intensity a first rough estimate regarding the relative fraction of rigid PVC at 150 °C can easily be made. For this purpose the relative fraction of the integral intensity represented by the broad resonance at 58.5 ppm (about $2B$, see Figure 5b) is compared to the total integral intensity of the −CHCl− resonance (A): $2B/A$. It is clear that this method is crude and only possible at the highest temperatures because of serious overlap between the broad and narrow resonances at temperatures below 150 °C. Nevertheless, the value of 0.14 determined in this way is in good agreement with the one obtained from the more accurate least-squares adjusted 2D best fit, as can be seen in Figure 6 where the rigid fraction resulting from the 2D fits is plotted as a function of temperature for the two samples studied. The figure clearly shows that the fraction of rigid PVC (rigid on the time scale of the single pulse NMR experiment), as represented by the broad resonances, gradually decreases with increasing temperature. It is also notes that the fraction of rigid PVC in

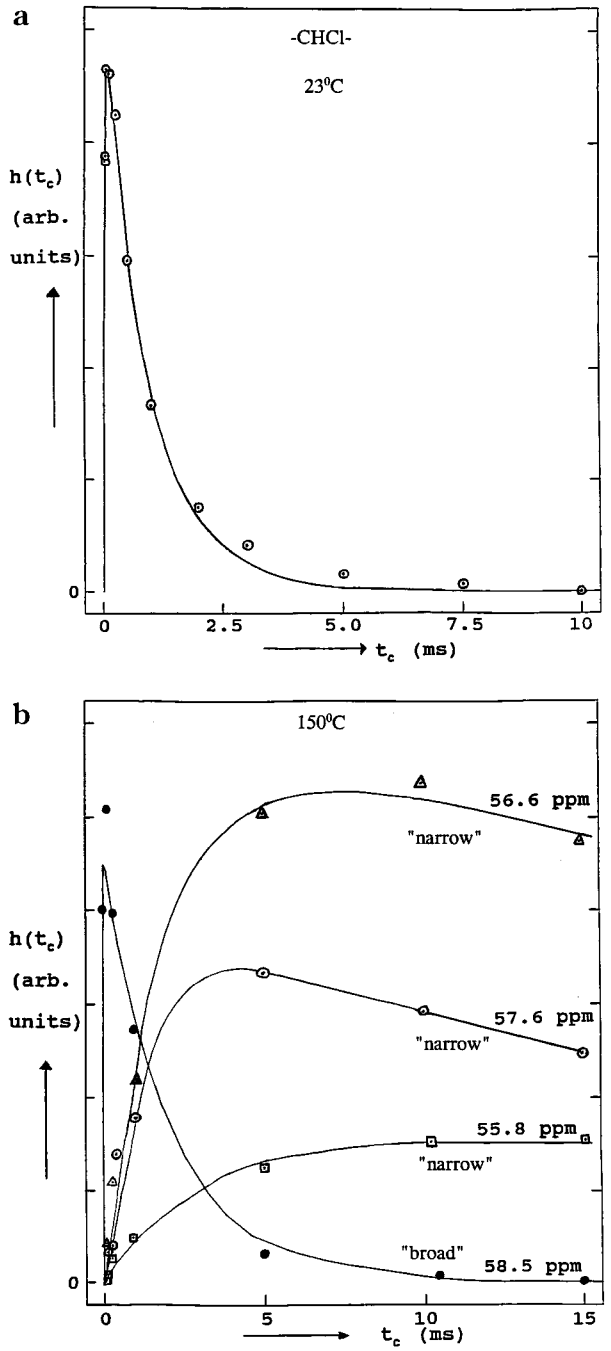

Figure 4. Signal intensity of the −CHCl− resonance(s) of sample 2 at (a) 23 and (b) 150 °C as a function of cross polarization time. The relative errors are about 10% and 25% from narrow and broad peaks, respectively.

the samples 1 and 2 is comparable throughout the whole temperature region.

In principle, the complete 2D fit analysis as carried out above for the −CHCl− region could also be performed for the $-CH_2-$ region since this region also shows broad and narrow peaks up to 180 °C. Above 150 °C the "multiplicity" of these peaks agrees with the number of peaks observed in the solution NMR spectrum (Figure 1), but below this temperature line, broadening seriously complicates a 2D fit analysis. In Figure 7 the $-CH_2-$ region of the ^{13}C spectrum at 180 °C is reproduced, together with the ^{13}C solution spectrum for comparison.

The quantification of each peak by the least-squares adjustment of the spectrum in Figure 7 suffers from relatively large uncertainties due to the strong overlap of the various peaks, in combination with the relatively large number of peaks. To reduce the experimental error, the least-squares adjusted parameters from the spectra at 165 and 180 °C are averaged, and in Table 2 all integral intensities of the various peaks, assuming Lorentzian line shapes, are tabulated. The results obtained from the ^{13}C solution spectrum are also included in the table. It is seen that the −CHCl− (Figure 6) and $-CH_2-$ (Table 2) regions yield similar values for the relative amount of rigid material at 160−180**E**C although the amounts in the $-CH_2-$ region are somewhat higher, which could be due in part to the fact that the results in the $-CH_2-$ region are less accurate than those in the −CHCl− region.

3.3. ^1H T_2 Relaxation. By means of a combination of solid-echo and Hahn-echo experiments it was found that the proton relaxation decay consists of three distinct components at temperatures well above (>50 °C) the glass transition temperature (at about −20 °C). The shortest T_2 value was observed by means of a solid echo pulse sequence. In Figure 8 a solid echo decay, starting at the top of the echo, is shown at 100 °C.

A statistically relevant best fit of the decay could be obtained by assuming a two component decay: a Gaussian for the fast decaying component and a Weibull function for the remaining relatively slowly decaying component. The T_2 of the fast decaying component is 20 μs, which is characteristic of a rigid amorphous phase below its glass transition and/or of a crystalline phase.[31,32] Apparently, the limited homogeneity of the permanent magnetic field of the spectrometer and the microscopic heterogeneity in the magnetic susceptibility in the sample do not allow accurate determination of the T_2 values for the mobile PVC and the DOP separately by means of the solid-echo experiment. Therefore the T_2 values for the two other components (intermediate and long components, T_2^{interm} and T_2^{long}, respectively) were determined with a Hahn-echo sequence which does not detect the fast decaying component. The measured curves above 0 °C were least-squares parameter adjusted to several possible functions consisting of two components. The statistically most relevant description of the decay above about 100 °C proved to be either a double exponential decay or a combination of a Cohen−Addad model for the intermediate component and an exponent for the slow one.

The decay rates and the relative amounts of the two components as obtained from the two models are very similar. In Figure 9a the results are therefore combined, and the differences resulting from the application of the two models are indicated by error bars.

It is seen that at temperatures below the glass transition (<−20 °C), the decay is characterized by only one short T_2. The glass transition (on the time scale of the NMR experiment, i.e., 10−100 μs), which manifests itself as a sharp increase in T_2, is observed at about −20 °C. Above about 30 °C, the increase in T_2 as a function of temperature is strongly different for the two components. Up to 180 °C, T_2^{long} increases by about an order of magnitude whereas T_2^{interm} increases only by a factor of 2. The range of T_2^{interm} values is typical for elastomers, and it will be shown below that this relaxation time is comparable to the T_2 of the amorphous PVC/VA copolymer whereas T_2^{long} is typical for the relaxation of relatively small organic molecules such as DOP.[32] It should be noted here that the difference in T_2 relaxation

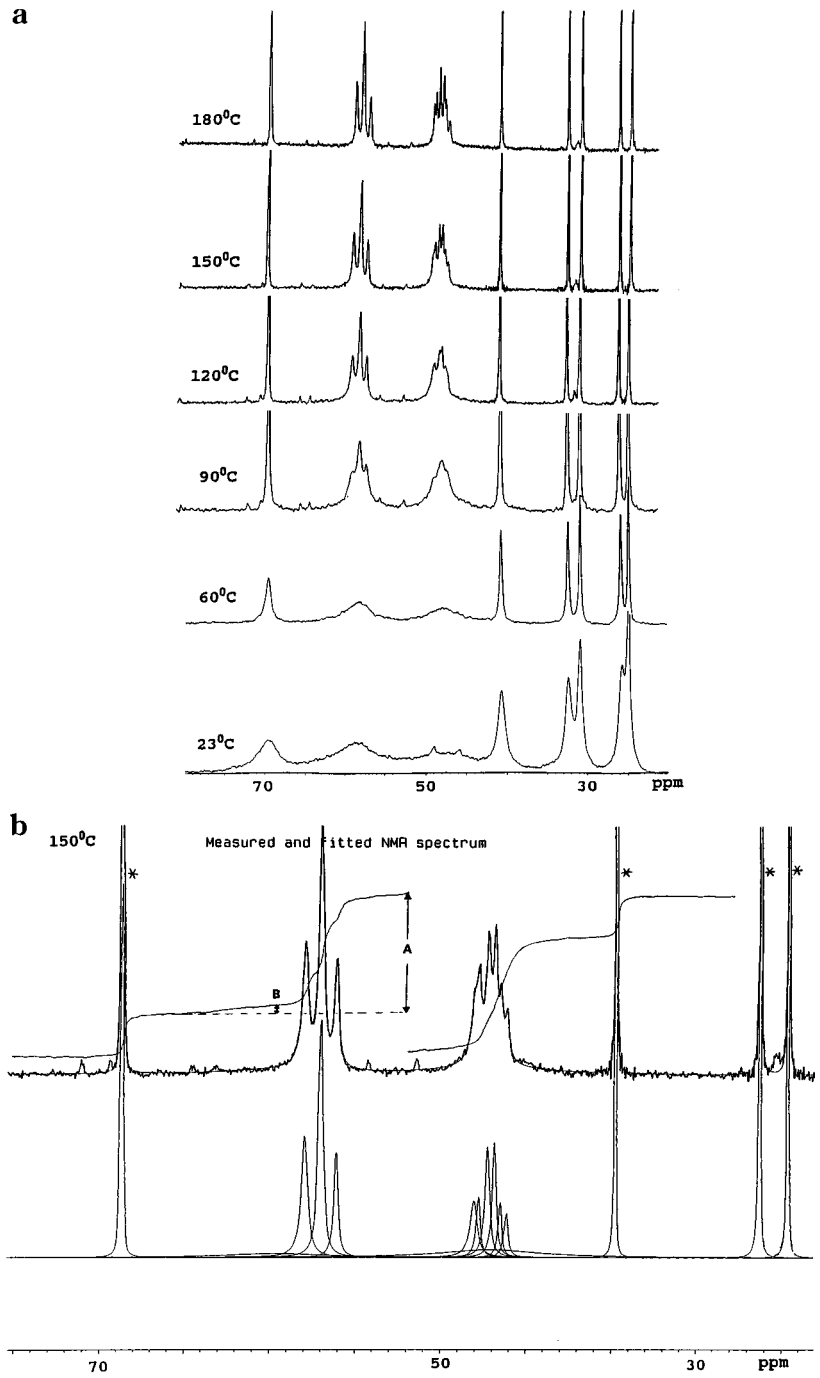

Figure 5. (a) 90° pulse ^{13}C HPPD spectra of sample 2 with a waiting time between consecutive pulses of 50 s at temperatures between 23 and 180 °C. (b) Constituent peaks from one of the spectra at 150 °C, resulting from a least-squares adjusted 2D best fit of a series of spectra having a different waiting time, are reproduced. The best fit is indicated by the curve drawn through the measured spectrum in the upper part of the figure. Above the measured spectrum, the integral intensity, as determined from the spectrum, is reproduced, from which a rough estimate regarding the relative amount of the integral intensity of the broad resonance at 58.5 ppm (equal to about 2*B*) with respect to the total integral intensity of the −CHCl− resonance (*A*) can be obtained. DOP resonances are marked by an asterisk.

time between mobile PVC and DOP does not imply the existence of separate phases of DOP and PVC since the T_2 is determined by the character of the motion (type, amplitude, and frequency) as well as by the chemical structure of the local surroundings.

In Figure 9b the relative fraction of the intermediate component is plotted as a function of temperature. Since this relative fraction is proportional to the total amount of protons in PVC with respect to that in DOP, it should reach 33% in the case where all the PVC material is amorphous. It is seen that the relative fraction of the intermediate component slowly increases toward about 33% as a function of temperature, which is indicated by the dashed line (the proton fraction of PVC). If we assume that the difference between the amount indicated by the dashed line and the observed amount is caused by a fraction of (in this Hahn-echo experiment) unobservable rigid component, an indirect estimate of the amount of rigid component can be made. According to the above results, the fraction of rigid PVC is about 35% at 100 °C and decreases to about 10% at 180 °C. Although this fraction at 100 °C is somewhat higher

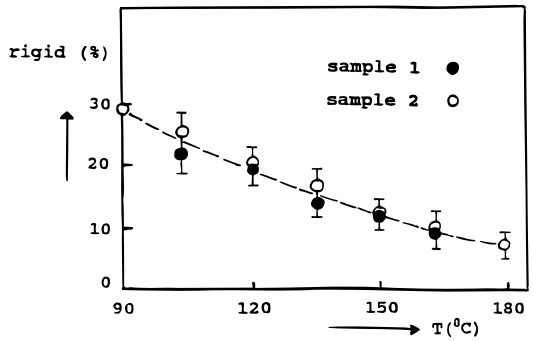

Figure 6. Fraction of rigid PVC as determined from the relative surface area of the broad 58.5 ppm peak for PVC/DOP (samples 1 and 2).

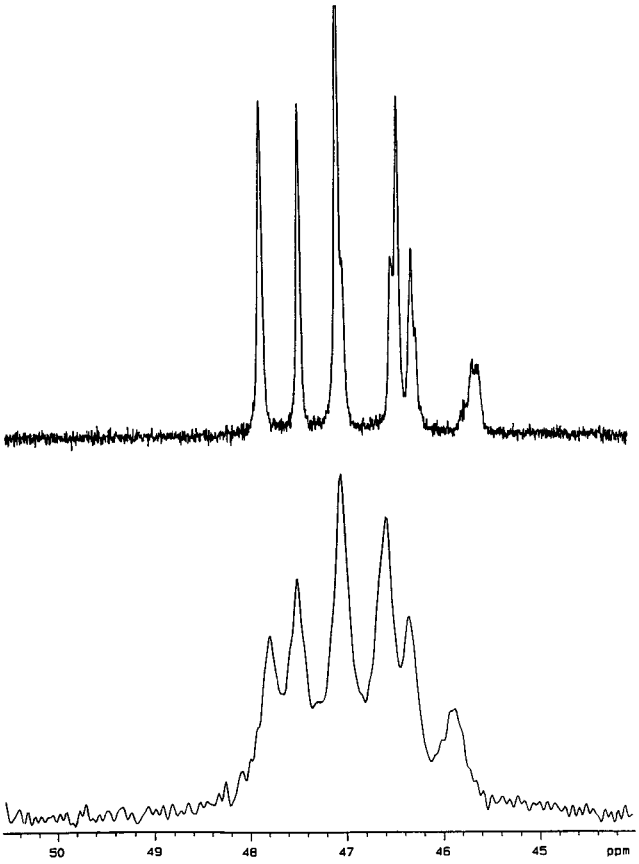

Figure 7. $-CH_2-$ region in a ^{13}C MAS NMR HPPD spectrum at 180 °C. At the top a ^{13}C solution spectrum is reproduced for comparison. The assignments are based on ref 17.

Table 2. Integral Intensity of the Broad ("Rigid" Phase) and Narrow Peaks ("Mobile" Phase) in the $-CH_2-$ Region (Sample 2) at 165 and 180°C

		mobile				
T (°C)	rigid	*rrr*	*rmr*	*mrr*	*mrm*/*mmr*	*mmm*
165	0.140	0.134	0.140	0.215	0.296	0.072
180	0.084	0.159	0.129	0.248	0.295	0.085
av	0.112	0.147	0.135	0.232	0.296	0.079
soln		0.187	0.144	0.269	0.315	0.085

than estimated on the basis of ^{13}C MAS NMR at 100 °C (see Figure 6), the agreement is relatively good, taking into account the experimental errors in the determination of the amount of "missing" rigid component in the proton decay. An alternative estimation of the amount of rigid material can be obtained from the solid echo decay in Figure 8. The normalized relative fractions of both decay functions at 100 °C are 0.07 and

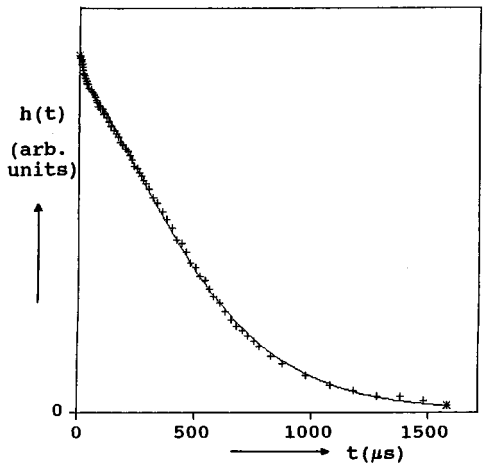

Figure 8. Decay of the transverse proton magnetization as measured by a solid-echo pulse sequence at 100 °C (points) for PVC/DOP (sample 2). The solid curve represents a least-squares fit of the decay using a linear combination of a Gaussian and a Weibull decay function.

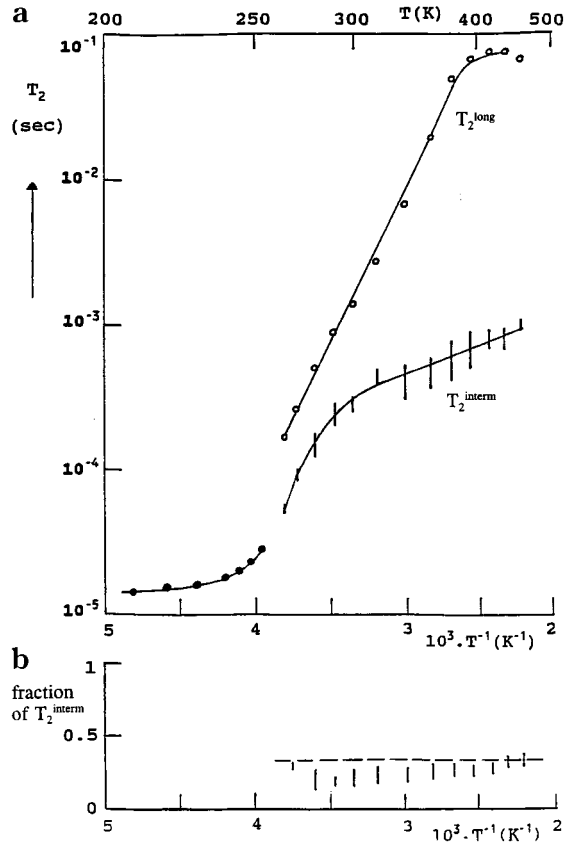

Figure 9. Temperature dependence of ^1H T_2 relaxation times (a) and the relative proton fraction of the intermediate relaxation component (b), as measured by the Hahn-echo experiment for PVC/DOP (sample 2). The fraction of the intermediate component is seen to approach the value of 0.33 at higher temperatures (dashed line). This value corresponds to the fraction of PVC protons in a 50/50 wt % mixture of PVC with DOP.

0.93 for the fast and (intermediate + slow) decay, respectively. Taking into account a PVC proton fraction of 0.33, a fraction of 0.21 of the PVC would be rigid. This fraction should be considered as a lower limit because of the relatively long 2τ value in the solid-echo pulse sequence (36 μs), which is on the order of the T_2 of this fraction.

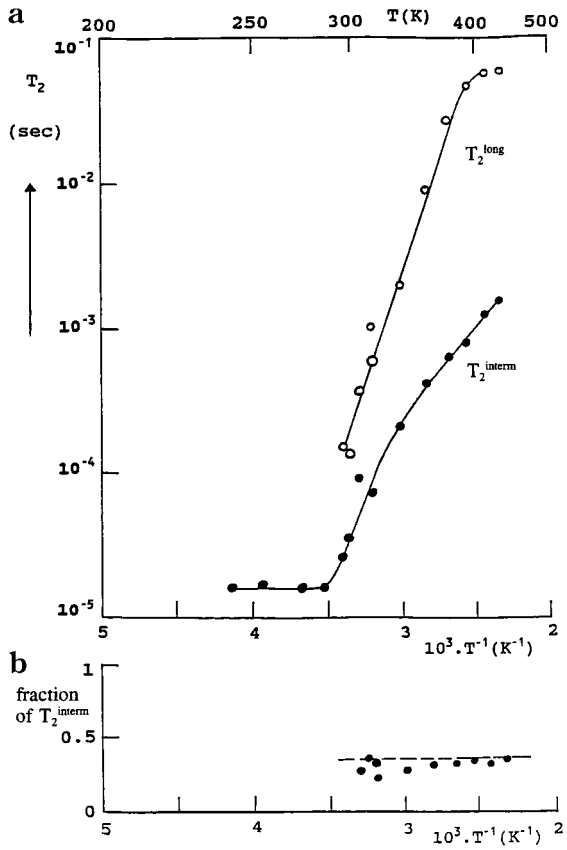

Figure 10. The ^{1}H T_2 (a) and the relative proton fraction of the intermediate relaxation component (b) for (PVC/VA)/DOP as a function of temperature.

To further explore the nature of the short component and to obtain information on the evolution of the intermediate component as a function of temperature, additional measurements on a reference for "truly amorphous PVC", a sample of a 50/50 wt % (PVC/VA)/DOP, were carried out. All decays were least-squares adjusted in the same way as for the PVC/DOP sample. According to Figure 10a the glass transition temperature is about 40−50 °C higher than that in the PVC/DOP sample. Above the glass transition, no short T_2 could be detected by the solid-echo experiment in this sample, and the decay consisted of only two components (as measured by the Hahn-echo experiment), i.e., the intermediate and the slowly decaying component, confirming the "fully amorphous" nature of the sample. Second, it is clearly observed in Figure 10a that above the glass transition T_2^{interm} increases much faster as a function of temperature than in PVC/DOP (Figure 9a).

The fraction of the intermediate component is furthermore equal to or close to 0.33 over the temperature interval above the glass transition.

4. Discussion

4.1. Two-Phase Structure of PVC/DOP. On the basis of the ^{13}C and ^{1}H NMR experiments as a function of temperature it appears that the PVC/DOP samples consist of two distinct (micro)phases. The chain mobility in these two phases is, at least at high temperatures, strongly different. On one hand, there is a rigid fraction of chains or chain segments characterized by broad ^{13}C resonances, short T_{CH} relaxation times, short $T_{1\rho}(^1H)$'s, relatively long ^{13}C T_1 relaxation times and short ^{1}H T_2 relaxation times. On the other hand there is a highly mobile fraction of chains or chain segments which appear as narrow peaks for the −CHCl− and $-CH_2-$ carbons in the ^{13}C spectrum, having relatively long T_{CH} values, long $T_{1\rho}(^1H)$ relaxation times, short ^{13}C T_1 values, and intermediate relaxation times in the proton experiments. The NMR relaxation behavior of the two fractions is typical of partially crystalline polymers.[31,32] No experimental result indicates a (significant) fraction of a possible "third phase" of intermediate mobility, which could be assigned to, e.g., a crystalline−amorphous interface. In the rest of this discussion we will therefore regard PVC as a two-phase system consisting of a rigid and a mobile PVC phase. The rigid fraction is thereby assumed to be completely due to crystallized chain units whereas the mobile fraction is assigned to the amorphous phase. It should be noted here that the term "crystallinity" should be treated with some caution since in the case of polymers such as PVC, where crystallites could be very small,[9,10] the value obtained for the degree of crystallinity can be technique dependent.

It is conceivable that in a 50/50 wt % PVC/DOP sample the DOP resides only in the amorphous phase and that the distribution of DOP in the amorphous phase is homogeneous.[9] The influence of DOP on the crystallinity cannot be estimated on the basis of the experiments described in this article. However, we are currently carrying out ^{2}H solid-state NMR experiments on deuterated PVC (without DOP), and preliminary results indicate similar amounts of rigid material as a function of temperature above the glass transition: about 20−25% at 90 °C to 10% at 125 °C.[33] We therefore assume that DOP acts as a type of solvent for the amorphous phase and it is reasonable to assume that crystals are formed at conditions close to equilibrium.

4.2. Crystallite Thickness. Knowledge of the degree of crystallinity and the contour length of the chains in the amorphous phase can provide information on the size of the crystallites along the chain direction. The proton T_2 experiments can provide useful information in this respect. Since the crystallites in PVC are thought to have very small dimensions along the direction of the chain, PVC at high temperatures can be regarded as an elastomer network in which the crystallites act as cross-links.[9,23,24] This view is in agreement with our T_2 observations of the PVC/DOP and the amorphous (PVC/VA)/DOP samples. For the amorphous (PVC/VA)/DOP sample above its glass transition, the rate of increase of T_2^{interm} as a function of temperature is qualitatively very similar to that observed for amorphous non-crosslinked polymers.[31,32] The PVC/DOP sample on the other hand shows a strongly reduced increase of T_2^{interm} as a function of temperature above its glass transition, suggesting the existence of "motional constraints" (physical "cross-links" or physical knots) in the amorphous phase. Because no real plateau, as observed in chemically cross-linked elastomers, is present, T_2^{interm} as a function of temperature can be qualitatively explained by a network in which the "cross-link" density decreases with increasing temperature.[9] This explanation also agrees with the ^{13}C results of a decreasing amount of rigid phase with increasing temperature, since the actual "cross-links" are considered rigid and the "cross-link" density is related to the amount of rigid (crystalline) phase.

Besides these qualitative considerations, a more quantitative picture can also be obtained. Using the

Table 3. Estimated Length of Amorphous Chain at 160 and 180 °C

T (°C)	$N_{\text{amorph+ent}}$	N_{amorph}
160	32	48
180	35	54

equations in section 2.4 (eqs 2 and 3) and the T_2^{interm} values, the number of monomer units (N) between crystallites and chain entanglements, $N_{\text{amorph+ent}}$, can be estimated at temperatures above 150 °C. Table 3 shows the results. The chain lengths represent an overall value in which the effects of chain entanglements, as they are present in the melt and possibly also (trapped) entanglements created by the crystallites, are also included. If we assume that only the type of entanglements which are present in the melt are important, i.e., that the measured value, $N_{\text{amorph+ent}}$, corresponds to a combination of the amorphous chain portions and the physical entanglements ($N_{\text{amorph+ent}}$), the chain length between crystallites can be estimated:

$$(N_{\text{amorph+ent}})^{-1} = (N_{\text{amorph}})^{-1} + (N_{\text{ent}})^{-1}$$

In doing so, we assume that network junctions arising from crystallites and the chain entanglements are decoupled and additive. For a chain entanglement density of about 100 monomers in the case of PVC in the melt,[28] the resulting chain length between crystallites is indicated in the Table 3 by N_{amorph}. If the average value of about 50 monomer units between cross-links is taken (average of N_{amorph} at 160 and 180 °C) in combination with the relative amount of crystalline PVC at 160−180 °C, the average number of monomer units along the chain direction in a crystallite can be obtained by assuming that $N_{\text{cryst}}/(N_{\text{amorph}} + N_{\text{cryst}})$ equals the relative rigid fraction as observed in Figure 6. For a relative amount of rigid (crystalline) PVC of 5−8%, a average number of 3−4 monomers is calculated. This means that the size of crystallites along the polymer backbone is very small, in agreement with the suggestions made by other authors.[10−12] It can be remarked here that the unusually small size of the crystallites (as compared to, e.g., polyethylene, polypropylene, etc.) may be the reason of the broadness of the broad "crystalline" resonance; i.e., since the surface of these small crystallites will be far from flat, there may be a broad distribution in carbon−proton local fields because of a relatively highly disordered crystalline phase. However, other reasons for its broadness, such as a broad distribution of correlation times in the intermediate mobility regime or effects of quadrupolar interaction with the chlorine atoms,[34,35] also cannot be excluded. From the NMR data it is not possible to estimate the crystallite size in the lateral chain direction, but according to X-ray measurements[10] platelets of about 40 Å on average exist in PVC. A minimum size of the crystallites in the lateral dimensions, is not known.

4.3. Tacticity of Crystallites. Information regarding the amount of crystalline phase and the tacticity in the crystallites can be obtained from the fully relaxed ^{13}C single pulse NMR spectra. The tacticity of the crystallites can be calculated from the integral intensities of the crystalline and amorphous peaks in the ^{13}C NMR spectra in combination with the "overall" tacticity as calculated from the ^{13}C solution spectra. In the following, the tacticity is derived for triad sequences but very similar equations can be derived for the case of tetrad

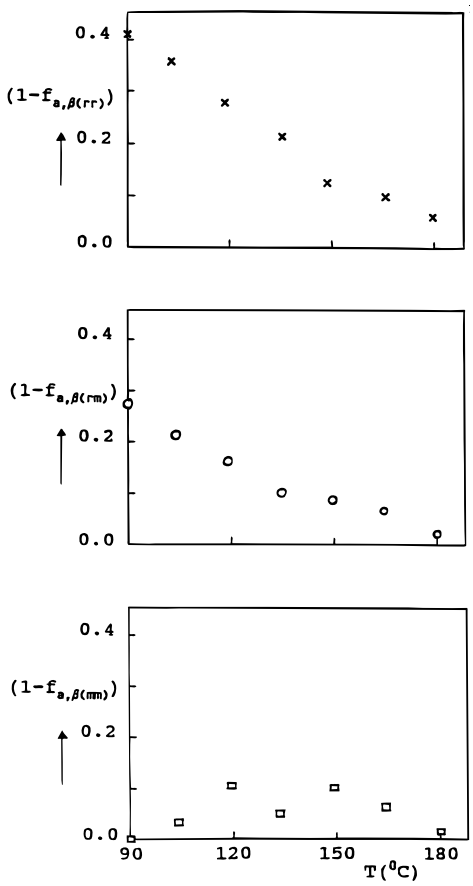

Figure 11. Fractions $(1 - f_{a,X})$ as a function of temperature for PVC/DOP as measured by ^{13}C NMR. For an explanation see eq 5 in the text.

sequences. From the ^{13}C solution NMR spectra the normalized fractions of the various triads are known (see Table 1) and must fulfill

$$\beta(rr) + \beta(rm) + \beta(mm) = 1 \tag{4}$$

Since we can assume PVC to be a two-phase system, a certain fraction $f_{a,X}$ ($X = \beta(rr)$, $\beta(rm)$, or $\beta(mm)$) of each type of chain unit with sequences rr, rm, and mm can be present in the amorphous phase and a fraction $(1 - f_{a,X})$ will reside in the crystalline phase. Assuming the two-phase model to be valid for semicrystalline PVC, we can then write

$$\beta(rr)f_{a,\beta(rr)} + \beta(rm)f_{a,\beta(rm)} + \beta(mm)f_{a,\beta(mm)} + \beta(rr)(1 - f_{a,\beta(rr)}) + \beta(rm)(1 - f_{a,\beta(rm)}) + \beta(mm)(1 - f_{a,\beta(mm)}) = 1 \tag{5}$$

Calculating the integral intensity of each amorphous −CHCl− peak divided by the total integral of the −CHCl− resonances (crystalline and amorphous), we obtain the fractions $f_{a,X}$, since X is known from the ^{13}C solution spectrum (see Table 1). This implies that the fractions of the various tacticities residing in the crystalline phase $(1 - f_{a,X})$ can also be obtained. In Figure 11 these fractions are plotted as a function of temperature. From this figure it is seen that the relative contribution of the triad $\beta(rr)$ in the crystalline phase is the largest of all three triads, followed by the relative contribution of $\beta(rm)$. $\beta(mm)$ has the lowest relative contribution, but it should be noted that the determination of this fraction suffers from larger errors than

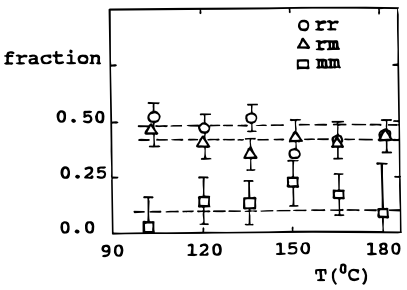

Figure 12. Triad tacticity of the rigid fraction of PVC/DOP, obtained from the least-squares spectral fitting results.

the other fractions due to the fact that the $\beta(mm)$ fraction is already low (about 0.2 for both samples), resulting in an "amplification" of errors by a factor of 5; see eq 5.

From the information obtained it is possible to estimate the relative content of each triad sequence in the crystallites (X^c; $X^c = \beta^c(rr)$, $\beta^c(rm)$ or $\beta^c(mm)$) by

$$X^c = X(1 - f_{a,X})/\Sigma X(1 - f_{a,X}), \qquad X = \beta(rr), \beta(rm), \beta(mm) \quad (6)$$

Similar calculations can be done for the tetrad and pentad sequences on the basis of the information given in Table 2. In the case of the averaged pentad sequences at temperatures of 165−180 °C, the following amounts of pentad sequences in the crystallites are obtained: *rrr* 36 ± 5%; *mrr*, 35 ± 10%; *mrm*/*mmr*, 16 ± 8%; *rmr*, 8 ± 8% *mmm*, 8 ± 8%. If we were to derive a maximum possible crystallinity from the tacticity of PVC, it would reach 0.70−0.75. For the triad sequences, the results for sample 2, which are identical to those for sample 1 within experimental error, are plotted in Figure 12. In this figure, the *rr* and *rm* triad contributions are about 0.5 and 0.4, respectively, whereas the *mm* triad contribution is nearly negligible within experimental error.

In terms of the syndiotactic tacticity of the crystallites (α^c), this would amount to 0.72, which is in agreement with the value found for the pentad sequences in the $-CH_2-$ region. If we compare this result with the syndiotacticity of the polymer of 0.56−0.58, it is first of all clear that there is a substantial enrichment of syndiotactic sequences in the crystallites. A second observation in Figure 12 is that the relative contribution of each chain sequence *rr*, *rm*, and *mm* does not seem to change, at least not significantly, over the whole temperature range. This constancy up to 180 °C suggests that the origin of the rigidity as observed by NMR is the crystallinity, because if part of the rigid fraction originated from some type of "rigid amorphous" phase (or heterogeneity in the DOP distribution), one would not expect the tacticity of this phase to remain constant over a wide temperature range. The constancy of the crystalline tacticity also suggests that crystallite perfection in terms of tacticity does not change as a function of temperature. This is rather surprising since it is often assumed that the very large melting range of PVC is connected with both the existence of a distribution of crystalline perfection and crystallite sizes, with the smallest and most imperfect crystallites melting at relatively low temperatures and the more perfect and/or largest crystallites melting at the higher temperatures.[4,36]

Since the gradual melting behavior is only borne out by the results of the relative amount of rigid material (see Figure 6) as a function of temperature, we suggest that crystallite perfection alone (in terms of a stereosequence distribution) is probably not a major parameter determining the melting temperature of a crystallite. The data therefore indirectly suggest that the size of the crystallites in the lateral chain direction is of major importance with respect to its melting temperature.

4.4. Statistical Analysis of the Chain Tacticity in Crystallites. On the basis of the same statistics as used in Flory's well-known theory of the crystallization of copolymers,[37] we can attempt to construct a micromorphological picture of PVC. The constraints which can help us to form this picture are the very small size of the crystallites along the chain direction and the tacticity data of the crystallites. The authors are aware that the crude assumptions made in Flory's model with respect to the chain statistics might result in an oversimplified picture.

It is first noted that the obtained "crystalline tacticity" of 0.72 (see section 4.3) does not indicate that *m* sequences are actually incorporated inside the crystallites, because if there are *m* sequences at the periphery of the crystallites, they will still be included in the observed NMR triad and tetrad sequences of the crystallites.

In the statistical model we also assume that crystals are constructed from *rr* sequences.

For the NMR application of the statistical model, which is dealt with in the appendix, we assume PVC to contain two types of chain sequences, i.e., racemic (*r*) and meso (*m*). Furthermore, only syndiotactic sequences (*rr*) above a certain minimum length (N_{min}) are taken into account as being crystallizable, which results in a distribution of crystallite thickness (as a consequence of the chain statistics) above this minimum length. Using these crude assumptions, the maximum relative amount of crystallizable sequences as well as the triad tacticities of the crystallites can be calculated. In Figure 13 the results of the model are shown as a function N_{min}. Figure 13a shows the calculated maximum number of crystallizable chain segments as a function of N_{min}.

It should be noted that the real amount of crystalline material should always be less than the values in Figure 13a since not every crystallizable chain segment will indeed crystallize, due to, for instance, a minimum size of the crystallites or the topological constraints imposed by the crystallites along the chains. The triad tacticities as obtained from the model are reproduced in Figure 13b. It is seen that they are strongly dependent on the crystallite thickness, which implies that this thickness can be estimated relatively accurately despite the relatively large error in the crystallite tacticity data as obtained from NMR. The value calculated from NMR (i.e. $rr \geq 0.5$ and $rm \approx 0.4$) agrees well with an N_{min} value of 3. The average number of monomer units in a crystallite (N_{av}, see Appendix) is then about 4, which agrees surprisingly well with the value of 3−4 derived from the ^1H relaxation experiments. This means that all the NMR results on the PVC/DOP samples can be simply explained by assuming that only syndiotactic sequences crystallize. Moreover, the limited number of monomers along the chain direction in the crystallites does not allow the incorporation of a substantial amount of *m* sequences into the crystallites[15,16] since this would strongly affect the average tacticity of the crystallites.

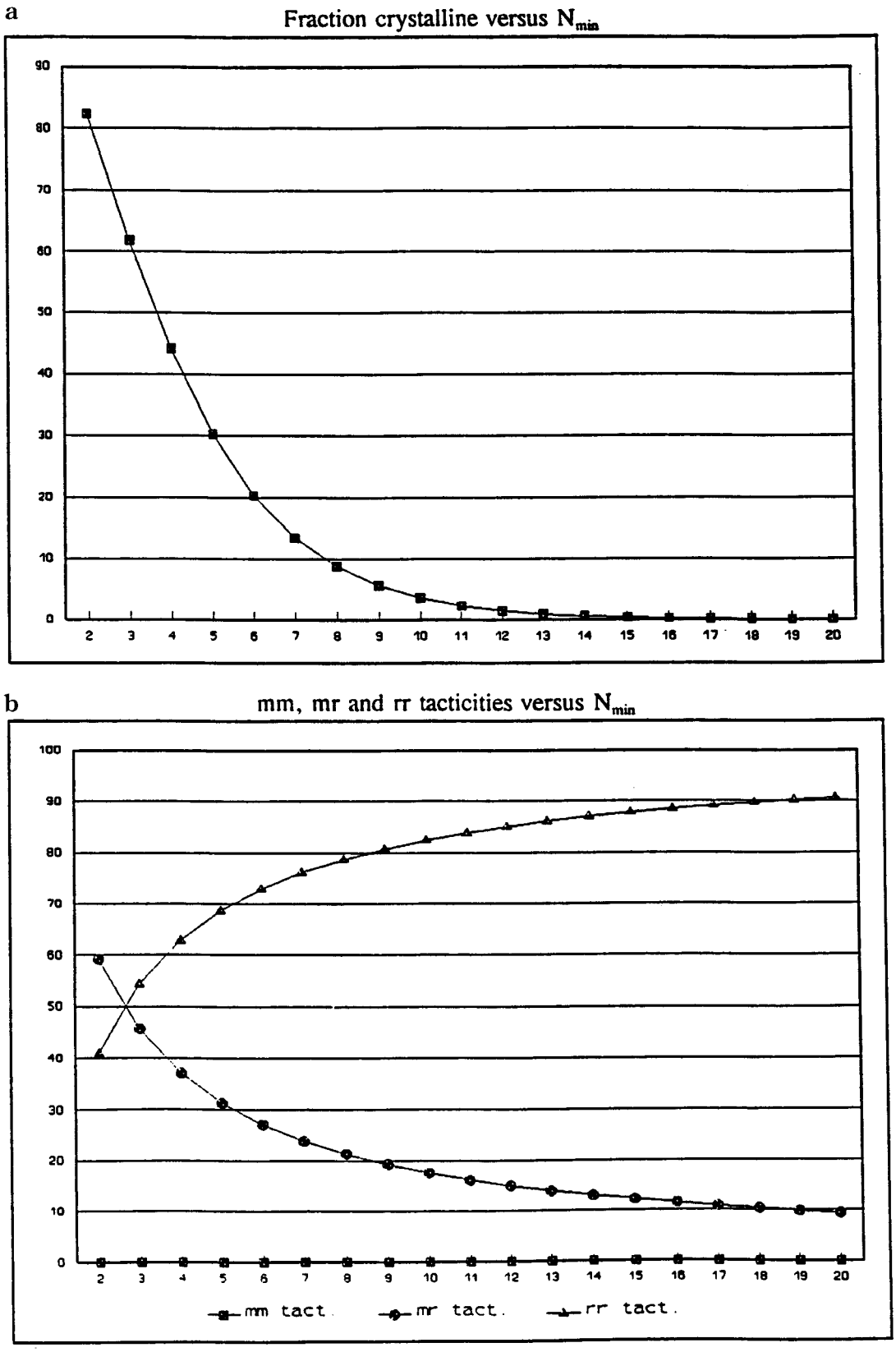

Figure 13. (a) Fraction of crystallizable material as a function of minimum syndiotactic sequence length obtained on the basis of the statistical model described in the appendix. (b) Calculated average crystallite triad sequences as a function of N_{min}.

5. Conclusions

In this article the relative amounts of rigid phase and the stereosequences in this phase in PVC/DOP samples were determined quantitatively as a function of temperature by means of solid-state NMR. On the basis of the NMR results PVC can be regarded as a two-phase system, i.e., crystalline and amorphous, since there are no indications of the existence of a third phase (interface). The degree of crystallinity, as determined with NMR, of the PVC/DOP samples is not strongly dependent on the tacticity. From the ^{13}C NMR experiments the tacticity of the crystalline as well as the amorphous

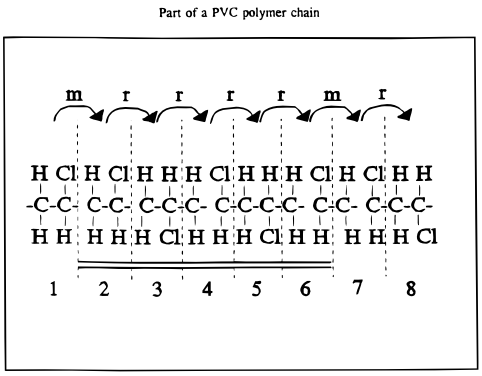

Figure 14. Simplified graphical representation of a *mrrrrmr* chain segment. The crystallizable segmental area is indicated by the double solid lines.

phase can be obtained as a function of temperature. From low-resolution proton relaxation experiments, an estimate of the amorphous chain length could be obtained which pointed to the existence of a crystallite thickness of only a few monomers at higher temperatures. All the observations can be well explained by chain statistics as used in Flory's model on the crystallization of copolymers, in which it is assumed that only syndiotactic sequences in PVC can be incorporated into the crystallites. On the basis of the results, it is conceivable that the large melting range in PVC is caused by the lateral size distribution of crystallites rather than by a distribution in crystallite perfection/tacticity.

Acknowledgment. The financial support for this research from LVM is gratefully acknowledged.

Appendix

To mimic the NMR results, we worked out the statistics as used in Flory's model in some detail regarding the tacticity of crystallites. Figure 14 shows a part of a PVC polymer chain consisting of 8 monomer units with the sequence *mrrrrmr*. The assumptions made in the model are the following:

(1) Only racemic sequences (=*r* sequences) are crystallizable. The overall chain fractions of syndiotactic sequences in the chain (obtained from solution NMR) is α.

(2) All crystallizable chains are assumed to crystallize. This means that the (syndiotactic) crystallites are terminated by one or more "*m*" sequences along the chain.

(3) If we have a sequence *mr...rm* (*n* times *r*), then (*n* + 1) monomers belong to the crystallite (double underlined monomers in Figure 14).

(4) A crystallized chain segment must contain at least $N_{min} > 1$ monomers.

(5) NMR detects (in the CHCl region) the mobile *mr*, *mm*, and *rr* sequences in the amorphous phase: it is assumed in the model that all *rr* sequences in the crystallite as well as the crystallite border sequences *mr* and *rm* are not detected as being mobile.

Taking into account the above assumptions it is possible to calculate the following parameters: f^c, the fraction of crystalline PVC, $\beta^c(rr)$, the fraction of *rr* sequences and $\beta^c(rm)$, $\beta^c(mm)$ the fractions of respectively *rm* and *mm* in the crystallites ($\beta^c(rr) + \beta^c(rm) + \beta^c(mm) = 1$).

Table 4. Fractions of f^c, f^{mm}, f^{mr}, f^{rr} and the Values of N_{av} Calculated, for Different N_{min} for $\alpha = 0.58$

N_{min}	N_{avg}	f^c	f^{mm}	f^{mr}	f^{rr}
2	3.4	47.8	0.0	59.2	40.8
3	4.4	35.9	0.0	45.7	54.3
4	5.4	25.6	0.0	37.2	62.8
5	6.4	17.6	0.0	31.3	68.7
6	7.4	11.8	0.0	27.1	72.9

All these fraction are dependent on N_{min}: the minimum number of monomers required in a crystallite along the chain direction.

We can write for f^c

$$f^c = \sum_{n=N_{min}}^{\infty} n \times \text{probability of the occurrence of a crystalline chain with } n \text{ monomers}$$

$$= \sum_{n=N_{min}}^{\infty} n \times \Pr(mr...rm)\{n-1 \text{ times } r\} = \sum_{n=N_{min}}^{\infty} n(1-\alpha)^2\alpha^{n-1}$$

$$= \alpha^{N_{min}-1}(N_{min}(1-\alpha)+\alpha)$$

For the fractions $\beta^c(mm)$, $\beta^c(rm)$, and $\beta^c(rr)$ we can derive

$$\beta^c(mm) = 0$$

$$\beta^c(rm) = \sum_{n=N_{min}}^{\infty} 2 \times \text{"probability of the occurrence of a crystalline chain with } n \text{ monomers"}$$

$$= \sum_{n=N_{min}}^{\infty} 2(1-\alpha)^2\alpha^{n-1} = \alpha^{N_{min}-1}2(1-\alpha)$$

$$\beta^c(rr) = \sum_{n=N_{min}}^{\infty} (n-2) \times \text{"probability of the occurrence of a crystalline chain with n monomers"}$$

$$= \sum_{n=N_{min}}^{\infty} (n-2)(1-\alpha)^2\alpha^{n-1} = \alpha^{N_{min}-1}(N_{min}) \times (1-\alpha) + 3\alpha - 2$$

The formulas for $\beta^c(mm)$, $\beta^c(rm)$, and $\beta^c(rr)$ as given above do not correspond to the definitions because these fractions are fractions of the total. To get the correct values, $\beta^c(mm)$, $\beta^c(rm)$, and $\beta^c(rr)$ have to be divided by f^c.

It is also possible to calculate N_{av}, the average length of crystalline chains:

$$N_{av} = \sum_{n=N_{min}}^{\infty} n \times \text{"probability of the occurrence of a chain with } n \text{ monomers, considering crystalline chains, only"} = N_{min} + \alpha/(1-\alpha)$$

For $\alpha = 0.58$ the calculated fractions (in %) f^c, f^{mm}, f^{mr}, f^{rr} and the values of N_{av} for different N_{min} are given in Table 4.

References and Notes

(1) Obande, O. P.; M. Gilbert, M. J. *Appl. Polym. Sci*. **1989**, *37*, 1713.
(2) Moore, W. H.; Krimm, S. *Makromol. Chem.: Suppl*. **1975**, *1*, 491.
(3) Guerrero, S. J.; Veleso, H.; Randon, E. *Polymer* **1990**, *31*, 1615.
(4) Illers, K. H. *J. Macromol. Sci.: Phys*. **1977**, *B14*, 471.
(5) Scherrenberg, R. L.; Reynaers, H.; Gondard, C.; Steeman, P. A. M. *J. Polym. Sci.: Polym. Phys.* **1994**, *32*, 111; Gilbert, M. *J. Macromol. Sci*. **1994**, *C34*, 77 and references therein.
(6) Scherrenberg, R. L. Thesis. The structural aspects of suspension poly(vinyl chloride). Catholic University, Leuven, Belgium, 1992.
(7) Scherrenberg, R. L.; Reynaers, H.; Gondard, C.; Verluyten, J. P. *Macromolecules* **1993**, *26*, 4118.
(8) Scherrenberg, R. L.; Reynaers, H.; Gondard, C.; Booij, M. *J. Polym. Sci.: Polym. Phys.* **1994**, *B32*, 99.
(9) Scherrenberg, R. L.; Reynaers, H.; Mortensen, K.; Vlak, W.; Gondard, C. *Macromolecules* **1993**, *26*, 3205.
(10) Summers, J. W. *J. Vinyl Technol*. **1981**, *3*, 107.
(11) Scherrenberg, R. L.; Reynaers, H.; Steeman, P. A. M.; Gondard, C. *J. Polym. Sci.: Polym. Phys*. **1994**, *32*, 119.
(12) Gray, A.; Gilbert, M. *Polymer* **1976**, *17*, 44.
(13) Carrega, M. *J. Pure Appl. Chem*. **1977**, *49*, 569.
(14) Gondard, C.; Scherrenberg, R. L.; Reijnaers, H. *Polymeric Materials Encyclopedia: Synthesis, Properties and Applications*; Salamone, J. C., Ed.; CRC Press. Inc.: Boca Raton, FL, 19XX.
(15) Juijn, J. A.; Gisolf, J. H.; de Jong, W. A. *Kolloid-Z. Z. Polym*. **1969**, *235*, 1157. Hobson, R. J.; Windle, A. H. *Makromol. Chem.: Theory Simul*. **1993**, *2*, 257.
(16) Juijn, J. A.; Gisolf, J. H. de Jong, W. A. *Kolloid-Z. Z. Polym*. **1973**, *251*, 456.
(17) Nakayama, N.; Aoki, A.; Hayshi, T. *Macromolecules* **1994**, *27*, 63.
(18) Torchia, D. A. *J. Magn. Reson*. **1978**, *30*, 613.
(19) Barendswaard, W.; Peters, E. To be published.
(20) Levenberg, K. *Q. Appl. Math*. **1944**, *2*, 164.
(21) Horii, F.; Hu, S.; Ito, T.; Odani, H.; Kitamaru, R.; Matsuzawa, S.; Yamaura, K. *Polymer* **1992**, *33*, 2299.
(22) Cohen−Addad, J. P.; Dupeyre, R. *Polymer* **1983**, *24*, 400.
(23) Mandelkern, L.; Edwards, C. O.; Domszy, R. C.; Davidson, M. W. *Polym. Sci. Techn*. **1985**, *30*, 121.
(24) Guerrero, S. J.; Keller, A.; Soni, P. L.; Geil, P. H. *J. Macromol. Sci.: Phys*. **1981**, *20*, 167.
(25) Gotlib, Yu. Ya.; Lifshits, M. I.; Shevelev, V. A.; Lishanskii, I. S.; Balanina, I. V. *Polym. Sci. USSR* **1976**, *18*, 2630.
(26) Fry, C. G.; Lind, A. C. *Macromolecules* **1988**, *21*, 1292.
(27) Simon, G.; Baumann, K.; Gronski, W. *Macromolecules* **1992**, *25*, 3624.
(28) Aharoni, S. M. *Macromolecules* **1986**, *19*, 426.
(29) Mirau, P. A.; Bovey, F. A. *Macromolecules* **1986**, *19*, 210.
(30) Voelkel, R. *Angew. Chem., Int. Ed. Engl*. **1988**, *27*, 1468.
(31) Fedotov, V. D.; Schneider, H. Structure and Dynamics of Bulk Polymers by NMR Methods. In NMR Basic Principles and Progress; Diehl, P., Fluck, E., Gunter, H., Kosfeld, R., Seelig, I. Eds.; Springer-Verlag: Berlin, 1989.
(32) McBrierty, V. J.; Packer, K. J. In *Nuclear Magnetic Resonance in Solid Polymers*; Davis, E. A., Ward, I. M., Eds.; Cambridge University Press: Cambridge, England, 1993.
(33) Barendswaard, W.; Litvinov, V. M.; Gondard, C. To be published.
(34) Andreis, M.; Koenig, J. L.; Gupta, M.; Ramesh, S. *J. Polym. Sci.: Part B, Polym. Phys.* **1995**, *33*, 1461.
(35) Harris, R. K.; Olivieri, A. C. *Prog. Nucl. Magn. Reson. Spectrosc.* **1992**, *24*, 435.
(36) Illers, K. H. *Makromol. Chem*. **1969**, *127*, 1.
(37) Flory, P. J. *Trans. Faraday Soc*. **1955,** 51, 848.
(38) Litvinov, V. M.; Barendswaard, W.; van Duin, M. *Rubber. Chem. Technol*. **1998**, *71*, 105.

MA971508Y